Cancer Chemother Pharmacol (2006) 58: 640–653
DOI 10.1007/s00280-006-0214-9

ORIGINAL ARTICLE

Chih-Chuan Chang · Yu-Chuan Liang
Athena Klutz · Chuan-I Hsu · Chien-Fu Lin
David E. Mold · Ting-Chao Chou · Yuan Chuan Lee
Ru Chih C. Huang

Reversal of multidrug resistance by two nordihydroguaiaretic acid derivatives, M_4N and maltose-M_3N, and their use in combination with doxorubicin or paclitaxel

Received: 24 October 2005 / Accepted: 11 February 2006 / Published online: 17 March 2006

Abstract *Purpose:* Multidrug resistance (MDR) continues to be a major obstacle for successful anticancer therapy. One of the principal factors implicated in MDR is the over expression of P-glycoprotein (Pgp), the product of the MDR1 gene. *Methods:* Here we explore the possibility of using the transcription inhibitor tetra-*O*-methyl nordihydroguaiaretic acid (M_4N) to inhibit Sp1-regulated MDR1 gene expression and restore doxorubicin and paclitaxel sensitivity to multidrug resistant human cancer cells in vitro and in vivo. *Results:* We found that M_4N acted synergistically with doxorubicin and paclitaxel in inhibiting the growth of the cells in culture allowing significant dose reductions of both drugs. We observed no such synergism when M_4N was used in combination with cisplatin, another chemotherapeutic agent, but not a Pgp substrate, as analyzed by the combination index and isobologram methods. Analysis of MDR1 mRNA and Pgp levels revealed that at sublethal doses, M_4N inhibited MDR1 gene expression in the multidrug resistant NCI/ADR-RES cells and reversed the MDR phenotype as measured by Rhodamine-123 retention. In addition, M_4N was found to inhibit doxorubicin-induced MDR1 gene expression in drug sensitive MCF-7 breast cancer cells. *Conclusions:* M_4N and maltose-tri-*O*-methyl nordihydroguaiaretic acid (maltose-M_3N), a water-soluble derivative of NDGA, were also able to reverse the MDR phenotype of the tumor cells in a xenograft model system and combination therapy with M_4N or maltose-M_3N and paclitaxel was effective at inhibiting growth of these tumors in nude mice.

Keywords M_4N · Maltose-M_3N · Multidrug resistance · Paclitaxel · P-glycoprotein · Xenograft

C.-C. Chang · Y.-C. Liang · A. Klutz · Chuan-I Hsu
C.-F. Lin · D. E. Mold · T.-C. Chou · Y. C. Lee
R. C. C. Huang (✉)
Department of Biology, Johns Hopkins University, 3400 N. Charles Street, Baltimore, MD 21218, USA
E-mail: rhuang@jhu.edu
Tel.: +1-410-5165181
Fax: +1-410-5165213

T.-C. Chou
Preclinical Pharmacology Core Laboratory, Memorial Sloan-Kettering Cancer Center, New York, NY 10021, USA

Introduction

A major obstacle in improving treatment results in breast cancer is the intrinsic or acquired resistance to cytotoxic drugs. One of the major mechanisms of drug resistance involves the over expression of a membrane protein, P-glycoprotein (Pgp), which is a member of the ATP-binding cassette (ABC) transporter family and is encoded by the MDR1 gene [1]. Pgp mediates the efflux from cancer cells of a variety of naturally occurring cytotoxic drugs including doxorubicin and paclitaxel. Doxorubicin is an anthracycline that interferes with DNA replication in rapidly dividing tumor cells by intercalating between DNA strands, disrupting the uncoiling of DNA by topoisomerase II and generating free radicals that cause DNA strand breaks [2]. Paclitaxel, a taxane, interferes with the depolymerization of microtubules, causing cell cycle arrest in mitosis and subsequent induction of apoptosis [3]. Anthracyclines and taxanes are among the most widely used adjuvant chemotherapeutic agents in the treatment of breast cancer, yet despite their effectiveness, resistance often develops resulting in the failure of chemotherapy.

A range of agents that reverse the multidrug resistance (MDR) phenotype and restore drug sensitivity to cancer cells has been developed [4]. First-generation MDR drugs, like verapamil (calcium channel blocker), cyclosporin A (immunosuppressant), quinine (antimalarial), progesterone (steroid hormone), and tamoxifen (antisteroid), have a relatively low affinity for MDR

transporters and possess other pharmacological activities which cause unacceptable side effects or toxicity at effective doses. Analogs of these drugs designed to eliminate their non-MDR pharmacological activities provided second-generation compounds like dextroverapamil and valspodar (a nonimmunosuppressive cyclosporine derivative). Unfortunately, these drugs also did not meet toxicity requirements. Third-generation drugs like elacridar, biricodar, zosuquidar, S-9788, and XR-9576 were designed de novo to have a high affinity for Pgp. These agents are currently under development and none has yet been approved for routine use. Other recent approaches to MDR reversal include the use of monoclonal antibodies against extracellular epitopes of Pgp [5], antisense and ribozyme nucleotides [6, 7] and RNA interference (RNAi) targeting MDR1 mRNA [8]. Such methods are limited by drug delivery issues.

Our approach to overcoming MDR1/Pgp-mediated MDR is unique in that it involves the use of a compound which itself is a potent anticancer agent. Tetra-*O*-methyl nordihydroguaiaretic acid (M_4N) is a nontoxic compound from the plant *Larrea tridentata*. Long-term toxicity tests for M_4N have been carried out in mice in two courses, 14 weeks [9] and 6 months [10] with an average oral uptake of 90 mg/mouse/day. There were no deaths and no significant body weight differences observed between control mice vs treated mice. In addition, M_4N treatment has caused no gastrointestinal disorders, anemia, or hair loss in dogs, rats, and rabbits [11] Nevertheless, M_4N has been shown to suppress the growth of a variety of mouse and human tumor cells and human tumor explants in nude mice [9]. Cancer cell growth retardation and cytotoxicity are the result of M_4N's ability to block binding of the transcription factor Sp1 to its cognate binding sites in the promoters of the Sp1-dependent genes CDC2 and survivin [12]. Inhibition of CDC2 expression leads to arrest at the G2 phase of the cell cycle [13]. Concomitant reduction and destabilization of survivin, an inhibitor of apoptosis protein (IAP), leads to death of the tumor cells [12].

Upregulation of global transcription in tumors has often originated from the hypoxia commonly known to exist in all tumors [14]. As a transcription inhibitor, M_4N might be expected to affect these genes in cancer cells as well. The MDR1 gene is activated by a diverse set of stimuli including the hypoxia-induced factor HIF-1α. These stimuli act on a region of the MDR1 promoter called the MDR1 enhancesome that includes binding sites for Sp1 and other members of the Sp family of GC-binding factors and transcription factor NF-Y [15]. Factors bound to the enhancesome recruit the histone acetyltransferase P/CAF that leads to chromatin remodeling and transcriptional activation. Because of its role in the MDR1 enhancesome, the Sp1/GC element interaction is an attractive target for therapeutic intervention. Based on this assumption we investigated whether M_4N could be used to reverse the MDR phenotype in multidrug resistant human cancer cells by inhibiting the Sp1-regulated expression of the MDR1 gene, thereby increasing the effectiveness of the cytotoxic drugs doxorubicin and paclitaxel. Because of M_4N's additional antitumor properties, combination therapy with M_4N and either doxorubicin or paclitaxel might be effectively carried out at reduced doses of both agents, thereby eliminating toxic side effects.

Materials and methods

Cell culture and drug additions

The human breast cancer cell line, MCF-7, was obtained from ATCC (Manassas, VA). The multidrug resistant cell line, NCI/ADR-RES, was obtained from the DTP Human Tumor Cell Line Screen (Developmental Therapeutics Program, NCI). Karyotyping analysis, DNA fingerprinting, and HLA genotyping have recently confirmed that the NCI/ADR-RES cell line is identical to the ovarian cell line OVCAR-8 [16]. Both cell lines were maintained in Dulbecco's modified Eagle's medium supplemented with 10% fetal bovine serum and the antibiotics penicillin and streptomycin. The NDGA derivative, M_4N, was synthesized as described previously [17]. Stocks of M_4N and paclitaxel (Sigma-Aldrich, St. Louis, MO) were prepared in dimethyl sulfoxide (DMSO) and added to the cell culture medium so that the final concentration of DMSO was 1%. Aqueous stocks of doxorubicin (Sigma-Aldrich) were prepared and filter sterilized before dilution into growth medium.

Cytotoxicity assay

NCI/ADR-RES and MCF-7 cells were seeded at a density of 2×10^4 cells per well in 24 well plates and 24 h later the growth medium was supplemented with M_4N, doxorubicin, paclitaxel, or combinations of M_4N with doxorubicin or M_4N with paclitaxel. M_4N was used at concentrations between 1.5 and 48 μM. For the combination of M_4N and doxorubicin, a constant molar ratio of 2.4:1 (M_4N:doxorubicin) was used, and for M_4N and paclitaxel the ratio was 20:1 (M_4N:paclitaxel). Three days after drug addition cytotoxicity was assessed with the SRB assay [18] with 540 and 690 nm (reference) absorbance measured with a Power Wave 200 microplate reader (Bio-Tek Instruments, Winooski, VT).

Evaluation of drug interactions

The combination index (CI) isobologram method of Chou and Talalay [19, 20], which is based on the median-effect principle, was used to calculate synergism or antagonism for the combined drug effects. Dose-effect curves for each drug, singly and in combination, in serially diluted concentrations were plotted using the median-effect equation and plot [21] and the CI equation

and plot [22]. CI values at different effect and dose levels and isobolograms were generated automatically using the computer software CompuSyn [23]. With this method, additive, synergistic, or antagonistic effects are indicated by CI values of 1, <1, and >1, respectively. Comparison of the ratio of doses required to reach a given effect level for each single drug and the drugs in combination was used to determine the dose-reduction index (DRI).

RT-PCR

Total RNA was isolated using the Trizol Reagent (Invitrogen, Carlsbad, CA). RT-PCR was carried out with the Superscript II One-Step RT-PCR system with Platinum *Taq* DNA Polymerase (Invitrogen) according to the manufacture's protocol using oligonucleotide primers specific for MDR1: 5′-ACATGACCAGGTATGCCT AT-3′, 5′-GAAGATAGTATCTTTGCCCA-3′ and GA PDH: 5′-CCATCACCATCTTCCAGGAG-3′, 5′-CCT GCTTCACCACCTTCTTG-3′.

The RT-PCR products were separated by agarose gel electrophoresis and stained with ethidium bromide. Relative band intensities were quantified by ImageJ software (NIH, Bethesda, MD).

Western blotting

Cultured cells were incubated in a solution of 10 mM EDTA and 10 mM EGTA in PBS and then harvested by scraping with a teflon cell scraper. The cells were pelleted and lysed in modified RIPA buffer [50 mM Tris-HCl (pH 7.4), 1% NP-40, 0.25% Na-deoxycholate, 150 mM NaCl, 1 mM EDTA (pH 8.0)] containing Protease Inhibitor Cocktail (Sigma Chemical Co., St. Louis, MO). The lysate was cleared by centrifugation, and protein concentrations were determined with the Bio-Rad Protein Assay (Bio-Rad Laboratories, Hercules, CA). Protein samples were separated by SDS-PAGE and electroblotted to a Hybond enhanced chemiluminescence (ECL) nitrocellulose membrane (Amersham Biosciences, Piscataway, NJ) with a semidry blotting apparatus and detected as described in the instruction manual of the ECL Western Blotting System (Amersham Biosciences). The antibodies used were primary rabbit polyclonal antibodies against Pgp and cyclin B and a horseradish peroxidase conjugated secondary antibody (Santa Cruz Biotechnology, Santa Cruz, CA). Relative band intensities were measured with ImageJ software.

Rhodamine-123 efflux assay

NCI/ADR-RES cells were cultured in the presence of 0, 1.25, 2.5, 3.75, and 5.0 μM M_4N. After 3 days, the cells were harvested by trypsinization and resuspended at a density of 5.0×10^6 cells/ml in the same media containing 1.0 μg/ml Rhodamine-123 (Sigma-Aldrich, St. Louis, MO). Following a 1-h incubation at 37°C, the Rhodamine loaded cells were washed twice with ice-cold PBS and resuspended in media with the starting concentrations of M_4N. During the efflux phase, 5.0×10^5 cells were collected every 15 min, washed in ice-cold PBS, resuspended in 100 μl of ice-cold PBS and analyzed by fluorometry at an excitation wavelength of 485 nm and an emission wavelength of 535 nm.

Synthesis of maltose-M_3N

Tri-*O*-methyl nordihydroguaiaretic acid (M_3N) was obtained from Dr. Jih Ru Hwu, National Tsing Hua University, Taiwan. It was mixed with an excess of *β*-maltose octa-acetate in dichloromethane and treated with boron trifluoride etherate for 3-4 h. After decomposition of the excess boron trifluoride, the organic solution was washed with cold solutions of sodium bicarbonate and sodium chloride, evaporated to syrup, and dissolved in 95% ethanol for chromatography on a column of Sephadex LH-20. The purified maltosylated M_3N was deacetylated in dry methanol with a catalytic amount of sodium methoxide, which was subsequently removed with Dowex 50×8 (hydrogen form). Evaporation of the methanolic solution yielded the final solid product.

Xenograft studies

T-cell deficient female nude (nu/nu) mice, 5–6 weeks of age, were purchased from Charles River Laboratories (Wilmington, MA) and were housed in a pathogen-free room. All experiments involving the mice were carried out in accordance with the Johns Hopkins University Animal Care and Use Committee guideline. The mice were implanted subcutaneously in both flanks with 1×10^6 NCI/ADR-RES cells suspended in Hank's balanced salt solution (HBSS). When the tumors exhibited a mean diameter of 2-4 mm, the mice were randomly assigned to the treatment groups that received M_4N alone or in combination with paclitaxel. For intraperitoneal (i.p.) administration, M_4N, maltose-M_3N, and paclitaxel were dissolved in a recently developed reduced cremophor solution containing 20% (v) dehydrated ethanol, 20% (v) Cremophor EL, PEG 300, $<11\%$ (v) Tween 80 [24]. Daily injections of 0.05 ml were performed for each drug and drug combination.

Tumors were measured in two perpendicular dimensions once every seven days, and the tumor volumes were calculated according to the following formula:

$$\text{Tumor volume} = (a^2 \times b)/2$$

where *a* is the width of the tumor (smaller diameter) and *b* is the length (larger diameter) [25]. The mean

tumor volume and standard error were calculated for each treatment group. Relative mean tumor volumes (V/V_0), where V is the mean tumor volume at a particular time and V_0 is the mean tumor volume at day 0 [26], were determined and used to assess tumor growth inhibition (T/C value) using the following equation:

$$\mathrm{T/C} = \text{Relative Mean Tumor Volume of treated/Relative Mean Volume of control} \times 100$$

The NCI standard for the minimal level for antitumor activity ($T/C \leq 42\%$) was adopted [25]. Differences between the relative mean tumor volumes of mice treated with the drug combinations and those treated with individual drugs were analyzed by the t-test. At the termination of the experiment, the tumors were excised and fixed in formaldehyde. Tissue samples were then sent to Paragon Bioservices (Baltimore, MD) for histology and immunohistochemistry using antibodies against human Pgp.

Results

Evaluation of the combined effect of M_4N and the chemotherapeutic agents, doxorubicin and paclitaxel

M_4N, doxorubicin, and paclitaxel, as single agents or in combination, inhibited the growth of the multidrug resistant human cancer cell line NCI/ADR-RES in a dose-dependent manner (Fig. 1a, b, Table 1). The average IC_{50} value for M_4N was 8.67 μM, while the IC_{50} values for doxorubicin and paclitaxel were 3.22 and 3.26 μM, respectively. The IC_{50} values for doxorubicin and paclitaxel are indicative of the MDR phenotype displayed by the NCI/ADR-RES cells as the reported IC_{50} values for these two agents are 130 and 6.4 nM for MCF-7, a drug sensitive human breast cancer cell line [27]. Conversely, the IC_{50} value for M_4N against MCF-7 from our previous studies [9] is approximately 7 μM, nearly the same as that for the drug resistant cell line. When used in combination in NCI/ADR-RES cells, M_4N and doxorubicin had IC_{50} values of 5.63 and 2.34 μM, respectively. For M_4N and paclitaxel in combination the IC_{50} values decreased to 3.31 (M_4N) and 0.17 μM (paclitaxel). To examine whether the effect of M_4N on doxorubicin and paclitaxel cytotoxicity is related to inhibition of Pgp activity, we performed two additional sets of experiments. One used M_4N in combination with cisplatin, a non-Pgp substrate. Another used M_4N in combination with the Pgp substrate doxorubicin in MCF-7 cells, which do not overproduce Pgp and are therefore drug sensitive. In both cases, the big decreases in the required dose for the IC_{50} of the second drug, paclitaxel for NCI/ADR-RES cells, doxorubicin for MCF-7 cells, was not observed (Fig. 1c, d, Table 1).

Two methods, the isobologram method and the CI method, were used to determine if there is synergy between M_4N and doxorubicin, paclitaxel, or cisplatin. Isobolograms were constructed for the doses of M_4N and doxorubicin, paclitaxel, or cisplatin necessary to inhibit growth 90% (Fa = 0.9), 75% (Fa = 0.75), and 50% (Fa = 0.5). The experimental data points for M_4N and doxorubicin and M_4N and paclitaxel drug combinations in the NCI/ADR-RES cells were at drug concentrations below the expected additive effect line for each of these values, indicating that there is a strong synergy (i.e., CI < 0.3) between M_4N and these two chemotherapeutic agents (Fig. 2A and B). Conversely, for the combination of M_4N and the non-Pgp substrate cisplatin, the data points were at drug concentrations at or slightly above the expected additive effect line, suggesting that there is no synergism between the two drugs (Fig. 2C). Similarly, there was no synergism indicated by the isobologram plot for M_4N and doxorubicin in the drug sensitive MCF-7 cell line (Fig. 2D).

The median effect analysis of Chou and Talalay [20] was also used to calculate the CI for each drug combination. In the drug resistant NCI/ADR-RES cell line, the M_4N and doxorubicin combination was very strongly synergistic (CI < 0.1) at high dose levels (ED_{90} and ED_{95}), whereas M_4N and paclitaxel were strongly synergistic (CI = 0.41–0.14) across the entire range of doses (Table 1 and Fig. 3A and B). When applied to the control experiments, with the combinations of M_4N and the non-Pgp substrate cisplatin in drug resistant cells and M_4N and doxorubicin in the drug sensitive MCF-7 cells, the median effect analysis revealed a markedly different situation. Both combinations across most of the range of doses were mildly antagonistic (CI = 1.1–1.6) (Table 1 and Fig. 3C and D).

The DRI determines the fold dose-reduction allowed for each drug in synergistic combinations. This is important since dose-reduction results in reduced toxicity while maintaining the desired efficacy. As a result of their synergism, the DRI exhibited a sizeable dose-reduction for doxorubicin and paclitaxel in the NCI/ADR-RES cells (Table 1). The DRI indicated that the concentration of doxorubicin necessary to inhibit the growth of NCI/ADR-RES cells by 75% (ED_{75}) could be decreased by 6.47-fold and that at the ED_{95}, it could be reduced by 87.56-fold. Similarly, the ED_{50} of paclitaxel could be decreased by 19.63-fold and the ED_{95}, by 300.34-fold. In contrast, the DRI for cisplatin in NCI/ADR-RES cells and doxorubicin in MCF-7 cells at ED_{50}, ED_{75}, ED_{90}, and ED_{95} ranged from 0.98 to 1.87 (Table 1). There was no dose-reduction advantage afforded by M_4N for non-Pgp substrate drugs or for drug treatment in cells lacking Pgp activity.

With the aim of demonstrating the effect of M_4N as a modulator of MDR and experimentally testing the theoretically determined reduction in the dose of doxorubicin, the IC_{50} of doxorubicin was determined in the

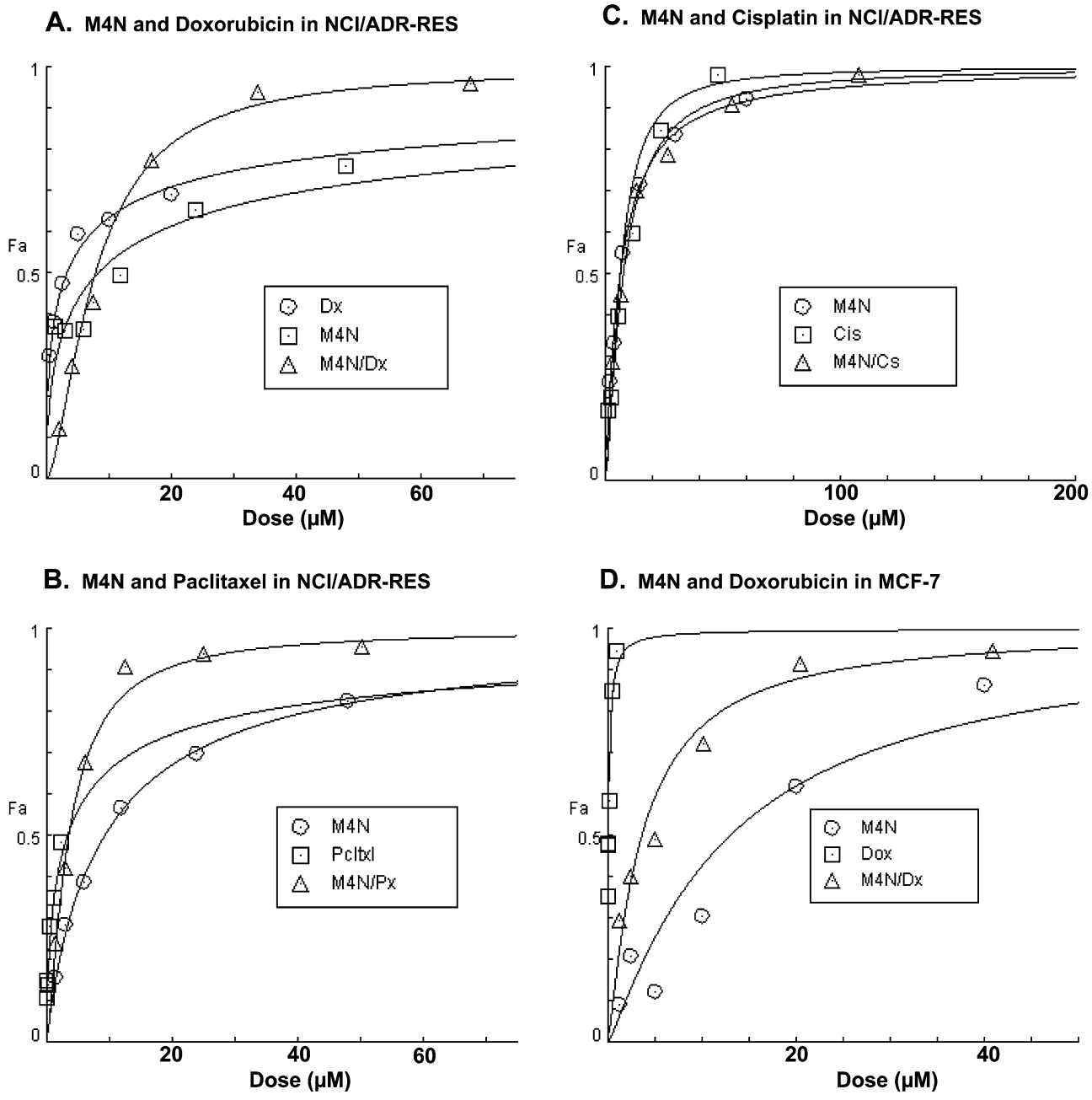

Fig. 1 Dose–effect curves for M_4N, doxorubicin, paclitaxel cisplatin and their combinations in NCI/ADR-RES and MCF-7 cells. **a** M_4N and doxorubicin (Dx), alone and in combination in NCI/ADR-RES cells. **b** M_4N and paclitaxel (Px), alone and in combination in NCI/ADR-RES cells. **c** M_4N and cisplatin (Cs), alone and in combination in NCI/ADR-RES cells. **d** M_4N and doxorubicin (Dx), alone and in combination in MCF-7 cells. The *x*-axis represents the dose of drug in μmol/l and the *y*-axis represents Fa, the fraction of cells affected (growth inhibition)

presence and absence of 25 μM M_4N. At this concentration of M_4N, there is a 65% reduction in the growth of NCI/ADR-RES cells. At this effect level of M_4N, the dose of doxorubicin can be theoretically reduced by 3.3-fold (data not shown). We found that the IC_{50} of doxorubicin in the absence of M_4N was approximately 32.5 μM, whereas in the presence of 25 μM M_4N the IC_{50} of doxorubicin decreased to about 5.1 μM (Fig. 4). This corresponds to a dose-reduction of 6.4 for doxorubicin, which correlates well with the theoretical value of 3.3. The increase in IC_{50} for doxorubicin in this experiment (32.5 μM), from what we previously observed for NCI/ADR-RES cells (3.22 μM, Table 1), is likely the result of the cells being plated at a higher initial cell density to counter the effects of the relatively high dose of M_4N.

Table 1 Dose-effect relationships of M_4N, alone and in combination with doxorubicin (Dox), paclitaxel (Px) or cisplatin (Cis) in human cancer cell lines

	Drugs	Parameters[a]			CI [b] (combination index) value at				DRI [c] (fold dose reduction) value at			
		D_m	m	r	ED_{50}	ED_{75}	ED_{90}	ED_{95}	ED_{50}	ED_{75}	ED_{90}	ED_{95}
NCI/ADR-RES	M_4N	8.19	0.52	0.92					1.46	5.94	24.3	63.2
	Dox	3.22	0.49	0.99					1.37	6.47	30.5	87.6
	M_4N/Dx	5.63 + 2.34	1.57	0.99	1.42	0.32	0.07	0.03				
	M_4N	9.14	0.91	1.00					2.75	3.98	5.76	7.40
	Px	3.26	0.59	0.97					19.6	54.3	150.3	300.3
	M_4N/Px	3.31 + 0.17	1.32	0.98	0.41	0.27	0.18	0.14				
	M_4N	6.24	1.07	1.00					1.47	1.79	2.17	2.48
	Cis	6.35	1.57	0.96					1.87	1.64	1.43	1.31
	M_4N/Cs	4.24 + 3.39	1.32	0.97	1.21	1.17	1.60	1.17				
MCF-7	M_4N	12.9	1.13	0.93					3.71	3.78	3.85	3.91
	Dox	0.09	0.96	0.94					0.98	1.18	1.43	1.62
	M_4N/Dx	3.49 + 0.09	1.15	0.98	1.29	1.11	0.96	0.87				

[a] D_m, median effect dose (concentration in micromoles/liter that inhibits cell growth by 50%) m shape of the dose-effect curve ($m = 1$, hyperbolic; $m > 1$, sigmoidal; $m < 1$, negative sigmoidal) R linear correlation coefficient of the median effect plot
[b] *CI* combination index (CI < 1, synergism; CI = 1, additive effect; CI > 1, atagonism)
[c] *DRI* dose reduction index (fold dose reduction indicated by the doses required to reach a given degree of inhibition when using the drug as single agent and in combination)

M_4N inhibition of MDR1 gene expression and Pgp levels in NCI/ADR-RES cells in culture

We next examined the effect of M_4N on MDR1 gene expression to determine whether the observed synergy between M_4N and doxorubicin and paclitaxel in multidrug resistant cells is the result of reversal of the MDR phenotype. Our original hypothesis was that M_4N, through its ability to inhibit Sp1-binding, might down regulate MDR1 gene expression. To examine this possibility, NCI/ADR-RES cells were exposed to 0, 5, 10, and 20 μM M_4N for 3 days, after which total RNA and protein were examined for levels of MDR1 mRNA and Pgp. After treatment with 20 μM M_4N, the level of MDR1 mRNA in the cells was reduced to 36.3% of the untreated value after normalization to the housekeeping gene GAPDH (Fig. 5A). The amount of Pgp was also reduced with its abundance decreasing to 17.8% of the control amount after a 3-day exposure to 20 μM M_4N (Fig. 5B). Even a 3-day exposure to 5 μM M_4N resulted in a 21.8% reduction in Pgp. The levels of Pgp were normalized to cyclin B1, whose expression, according to our previous results, is unaffected by M_4N [13].

The results indicate that M_4N may be able to reverse the MDR phenotype by inhibiting the constitutive expression of MDR1 mRNA and Pgp in multidrug resistant cells. Next, we investigated whether M_4N could be used to prevent cells from acquiring resistance after exposure to chemotherapy. MDR1 gene expression is induced when the drug sensitive human breast cancer cell line is exposed to low doses of doxorubicin. We treated MCF-7 cells for 2 days with 0.05 μM doxorubicin in the presence or absence of 5.0 μM M_4N and measured the relative amounts of MDR1 mRNA and Pgp protein. Treatment with doxorubicin in the absence of M_4N-induced measurable expression of both MDR1 mRNA and Pgp (Fig. 6). MDR1 expression was not detectable in MCF-7 cells without exposure to doxorubicin. Induction of MDR1 expression was abolished, however, by combination treatment with M_4N (Fig. 6).

Effect of M_4N on Rhodamine-123 efflux in multidrug resistant cells

Efflux of doxorubicin and paclitaxel from multidrug resistant cells is mediated by Pgp. The Pgp substrate Rhodamine-123 was used to examine the effect of Pgp down regulation by M_4N on drug efflux. The NCI/ADR-RES cells were incubated for 3 days in the presence of 0, 1.25, 2.5, 3.75, and 5.0 μM M_4N. The cells were then loaded with Rhodamine-123, washed and allowed to efflux with or without M_4N. During the efflux period, the cells were assayed for the amount of cell-associated Rhodamine-123 at 15 min intervals for an hour. Untreated resistant cells had an E_{50} (time at which 50% of Rhodamine-123 is retained by the cells) of approximately 12 min (Fig. 7). Treatment of cells with 1.25, 2.5, 3.75, and 5.0 μM M_4N increased the E_{50} to 12.5, 12.5, 15, and 20 min, respectively. These results, on slowing down the drug efflux, are consistent with the reduction of Pgp levels in cells by M_4N.

Combination therapy of M_4N or maltose-M_3N and paclitaxel against NCI/ADR-RES resistant cancer xenografts in nude mice

Nude mice bearing NCI/ADR-RES multidrug resistant cancer xenografts were used as a model for combination therapy to further examine synergy between M_4N and paclitaxel. Two dosage regimens of M_4N and paclitaxel,

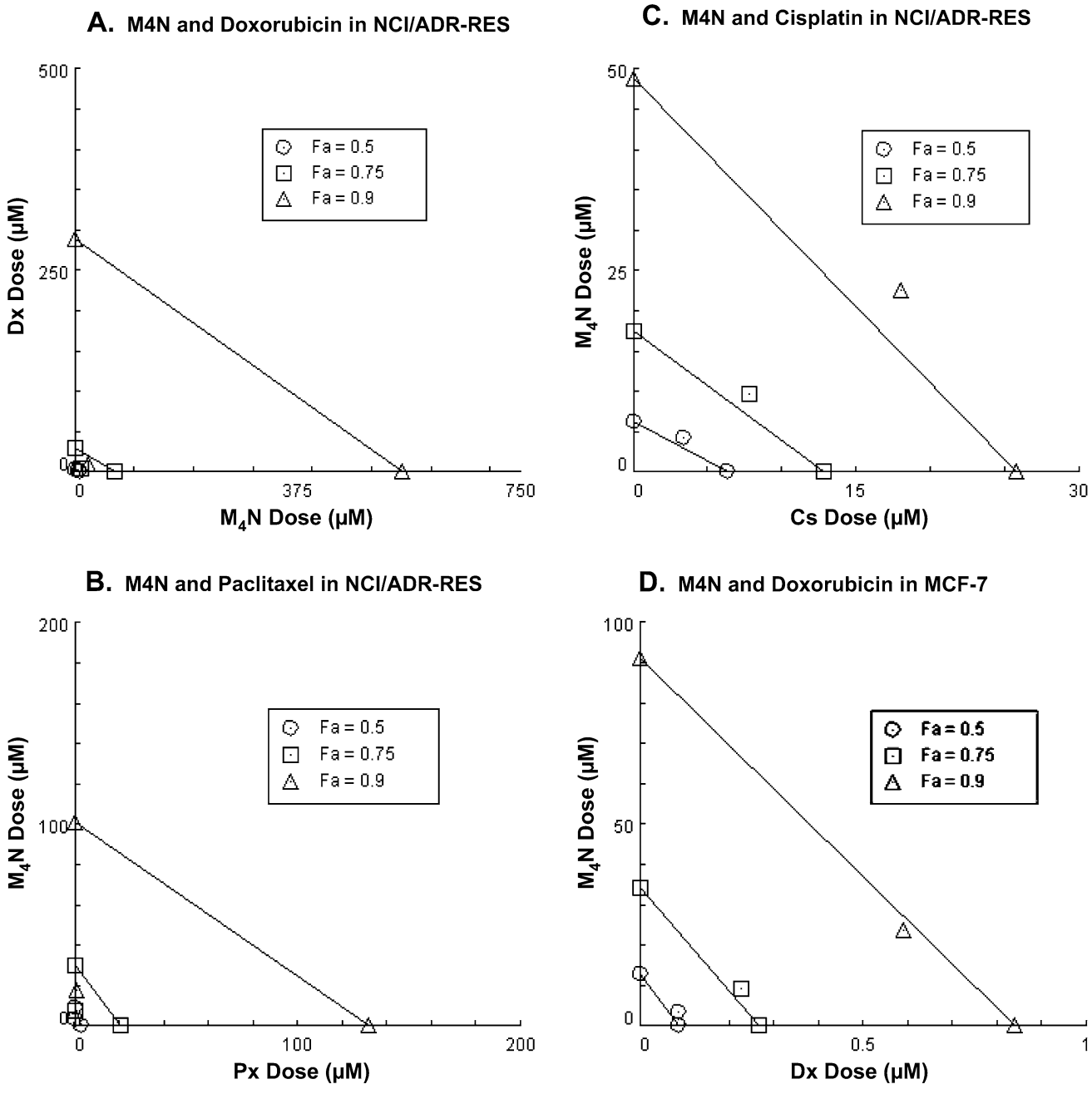

Fig. 2 Analysis of the combination of M_4N with doxorubicin, paclitaxel, or cisplatin in NCI/ADR-RES and MCF-7 cells at different effect levels (Fa). Isobolograms for **a** the combination of M_4N with doxorubicin (Dx) in NCI/ADR-RES cells, **b** the combination of M_4N with paclitaxel (Px) in NCI/ADR-RES cells, **c** the combination of M_4N with Cisplatin (Cs) in NCI/ADR/RES cells, and **d** the combination of M_4N and doxorubicin (Dx) in MCF-7 cells. Combination data points located on the hypotenuse, lower left, and upper right, represent additive effect, synergism, and antagonism, respectively

both with a constant molar ratio of 20:1 (M_4N:paclitaxel), were employed (Table 2). The 8 and 16 μmol/m^2 doses of paclitaxel were submaximal based on values from other studies [28], and the M_4N doses of 160 and 320 μmol/m^2 were arrived at by decreasing the maximum tolerated dose used in our previous study with MCF-7 breast cancer xenografts [9]. An additional NDGA derivative was also tested. Maltose-M_3N is being developed as a water-soluble alternative to M_4N, however, for consistency it was dissolved in the same reduced cremophor solvent system as M_4N and paclitaxel for this study. For control mice receiving the solvent only, the explanted tumors increased appreciably over 2 weeks of treatment, with the mean tumor volume nearly tripling in size (Table 2). Tumor growth was also noted in mice treated with submaximal doses of either M_4N

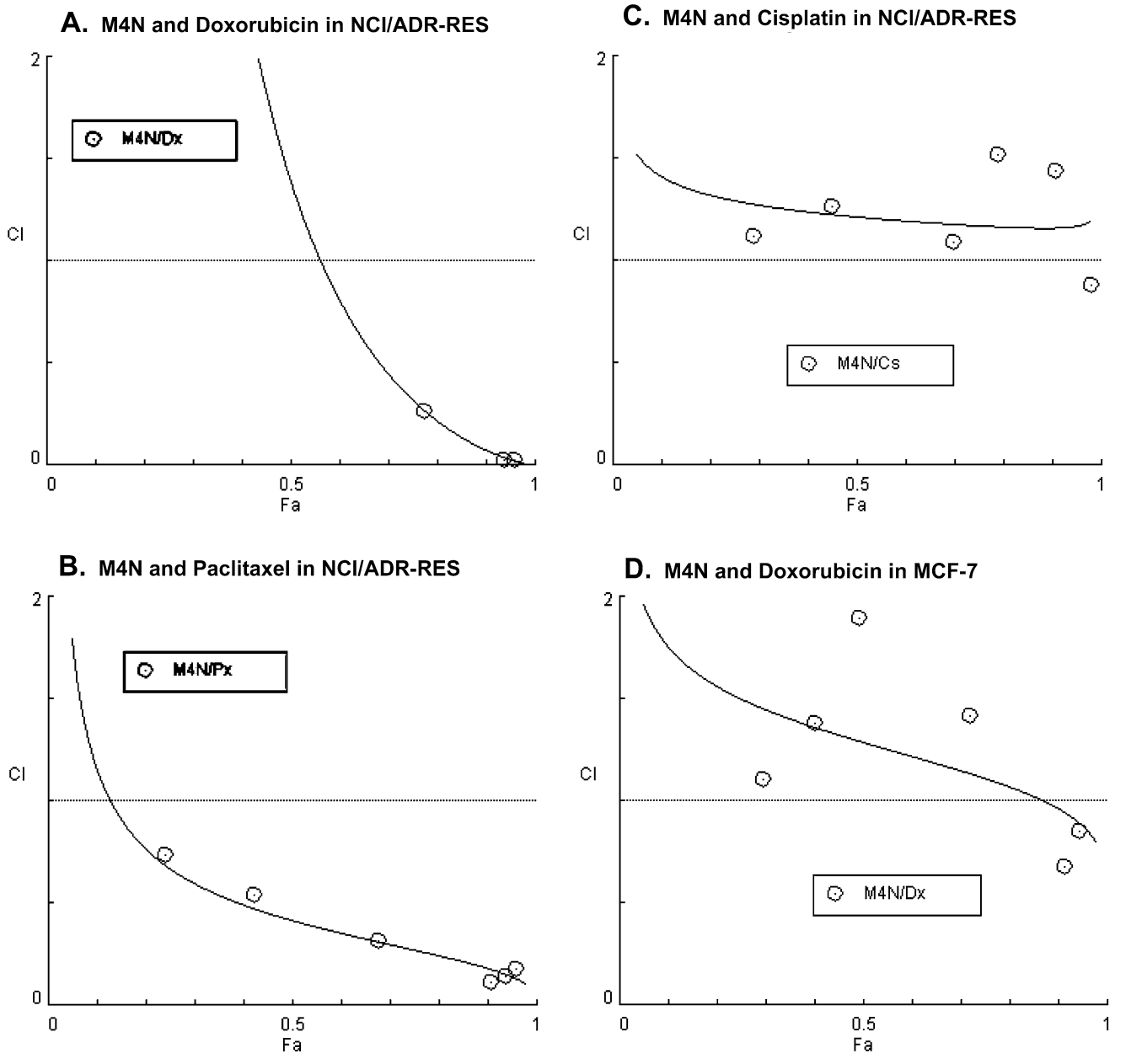

Fig. 3 Analysis of the combination of M_4N with doxorubicin, paclitaxel, or cisplatin in NCI/ADR-RES and MCF-7 cells. CI plots for **a** the combination of M_4N with doxorubicin (Dx) in NCI/ADR-RES cells, **b** the combination of M_4N and paclitaxel (Px) in NCI/ADR-RES cells, **c** the combination of M_4N and cisplatin (Cs) in NCI/ADR-RES cells, and **d** the combination of M_4N and doxorubicin (Dx) in MCF-7 cells. CI = 1, <1, and >1 indicates additive effect, synergism, and antagonism, respectively

(320 μmol/m^2), paclitaxel (16 μmol/m^2), or maltose-M_3N (320 μmol/m^2) with relative mean tumor volumes after 2 weeks of 1.33, 1.59, and 1.25, respectively. For the mice treated with a combination of M_4N and paclitaxel or maltose-M_3N and paclitaxel, however, the final relative mean tumor volumes were 0.94 and 0.65, respectively, indicating an overall decrease in tumor size (Table 2). Using the *t*-test these values are significantly lower than those for the individual drugs at the $P = 0.057$ level (paclitaxel vs M_4N/paclitaxel) and $P = 0.005$ level (paclitaxel vs maltose-M_3N/paclitaxel). Moreover, the tumor growth inhibition (T/C) values for each of the drug combination regimens were all lower than 42%, the minimum level for antitumor activity according to National Cancer Institute standards [25].

The health and well-being of the mice were assessed by recording their body weights at the beginning and end of the treatment period. For each of the dosage regimens, the mean change in body weight was small (−0.9 to +1.3) and not significantly different from that for the control group (Table 2). The only two treatment groups exhibiting a decrease in mean body weight were

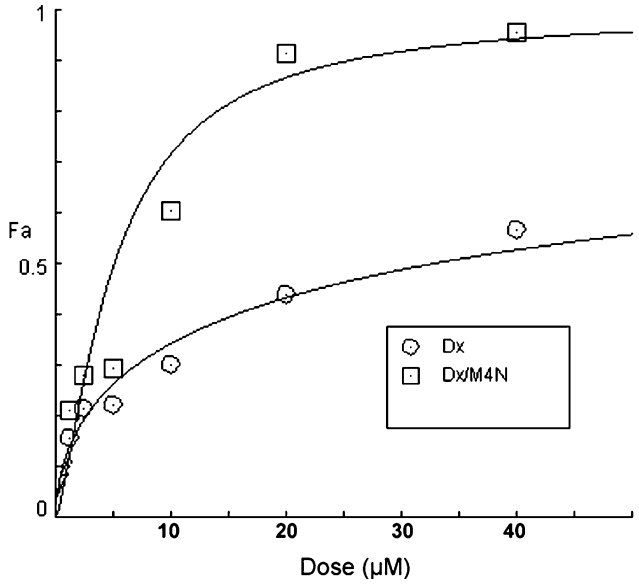

Fig. 4 Dose-effect curves for doxorubicin (Dx) in the presence and absence of 25 μM M_4N. The *x*-axis represents the dose of drug in μmol/l and the *y*-axis represents Fa, the fraction of cells affected (growth inhibition)

advantage of combination therapy with synergistic drugs is the ability to use submaximal doses of the chemotherapeutic agents. This is reflected in the decreased toxicity of the treatment regimens as illustrated by the stability of body weight and the zero mortality rate.

M_4N and maltose-M_3N inhibition of Pgp levels in NCI/ADR-RES breast cancer xenograft tumors

In order to examine the mechanism underlying the apparent synergism between M_4N and paclitaxel in inhibiting the growth of the drug-resistant xenografts, the tumors were analyzed for the presence of Pgp. Tissue sections from xenograft tumor biopsies from each of the treatment groups were stained with either hematoxylin and eosin (H&E) or immunochemically using Pgp-specific antibodies. Tumor sections from the control group exhibited robust antibody staining for Pgp at the surface of most of the tumor cells (Fig. 8). A similar pattern was seen in the paclitaxel treated tumors. In contrast, the M_4N and maltose-M_3N treated tumors showed a dramatic decrease in antibody staining consistent with a

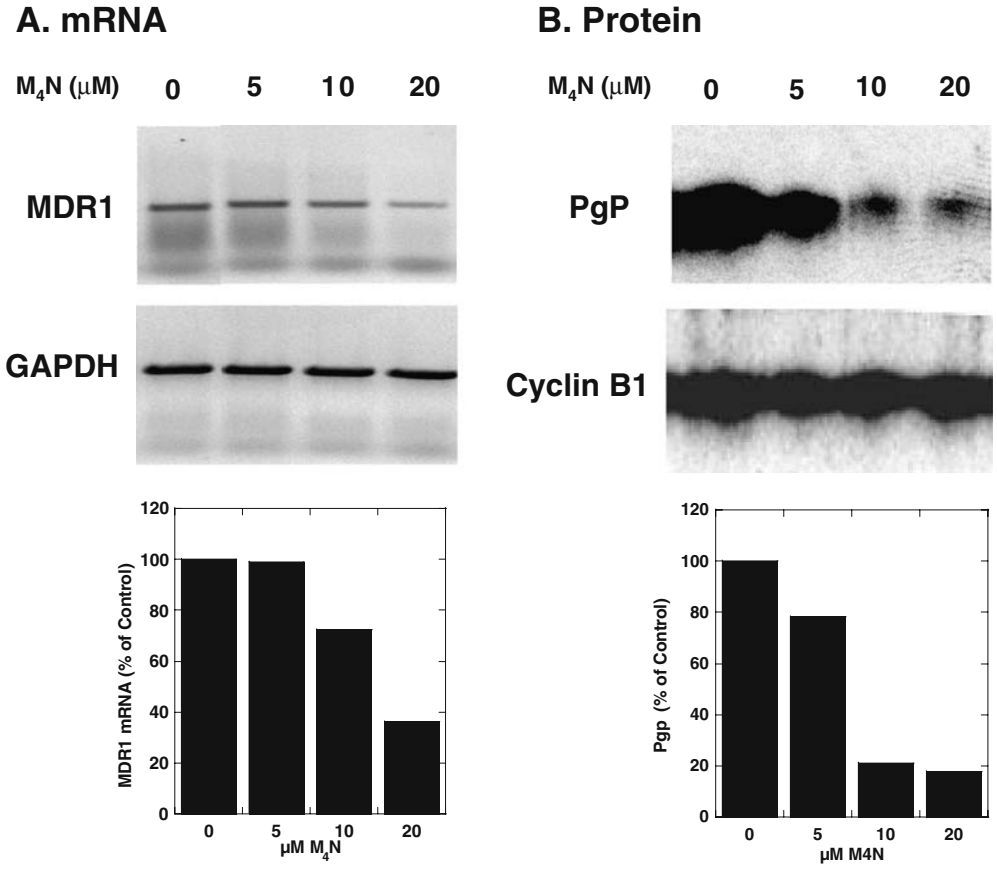

Fig. 5 Effect of M_4N on MDR1 gene expression and P-glycoprotein levels in NCI/ADR-RES human breast cancer cells. **a** Agarose gel analysis of MDR1 and GAPDH (normalization control) cDNAs generated by RT-PCR of total RNA from cells treated for 3 days with 0, 5, 10, and 20 μM M_4N. Results in bar graph form normalized to GAPDH. **b** Western blot analysis of Pgp and cyclin B1 (normalization control) protein levels in cells treated for 3 days with 0, 5, 10, and 20 μM M_4N. Results in bar graph form normalized to cyclin B1

the higher dose single drug regimens of M_4N and paclitaxel (−0.2 and −0.9, respectively). There were no mouse deaths recorded in any of the groups. An decrease in the amount of Pgp protein. Tumors treated with a combination of M_4N and paclitaxel showed tumor regression with some central necrosis as evidenced

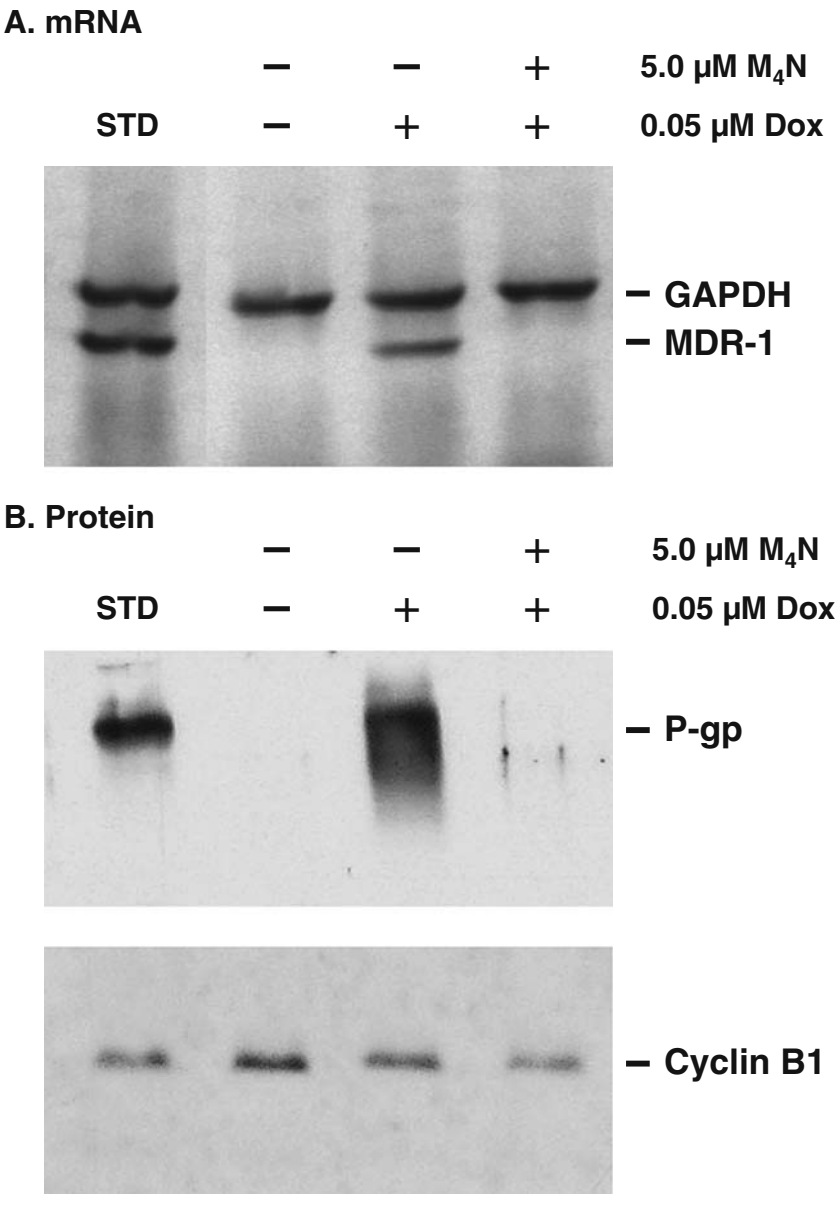

Fig. 6 Effect of M_4N on induction of MDR1 gene expression by doxorubicin in MCF-7 cells. MCF-7 cells were left untreated or treated with 0.05 μM doxorubicin in the presence or absence of 5 μM M_4N for 2 days and then total RNA and protein were analyzed for MDR1 gene expression and Pgp protein levels. **a** Agarose gel analysis of MDR1 and GAPDH (normalization control) cDNAs generated by RT-PCR. STD, cDNAs from NCI/ADR-RES cells. **b** Western blot analysis of Pgp and cyclin B1 (normalization control) protein levels. STD, analysis of proteins from NCI/ADR-RES cells

by H&E staining and an absence of Pgp antibody staining (Fig. 8). Pgp levels were similarly decreased in the maltose-M_3N/paclitaxel treated tumors.

Discussion

The first-generation of MDR reversal agents were pharmacologically active compounds that happen to also bind to Pgp. These drugs were ultimately unsuccessful because their other pharmacologic properties made them too toxic for clinical use. M_4N is uniquely suited to perform the task of resensitizing cells to chemotherapeutic drugs like doxorubicin and paclitaxel. Like verapamil or cyclosporin A, M_4N has pharmacologic activity beyond reversal of the MDR phenotype. In the case of M_4N, however, its other actions are beneficial to the primary goal of eliminating cancer cells. Our previous preclinical studies with M_4N has shown that it can successfully inhibit the growth of six different tumor types, including MCF-7 and NCI/ADR-RES cell-induced carcinoma, when administered systemically to nude mice, making it an attractive candidate for adjuvant chemotherapy [9, 29]. The results reported here demonstrate that M_4N, which is a transcription inhibitor for SP1-regulated MDR1 gene expression, effectively inhibits the growth of multidrug resistant tumor cells in cell culture and in vivo in human tumor xenografts. In combination with doxorubicin or paclitaxel, M_4N not only increases their effectiveness, but also contributes to cancer cell killing, thereby allowing significant reductions in the dose requirements for both doxorubicin and paclitaxel as well as the dose for M_4N.

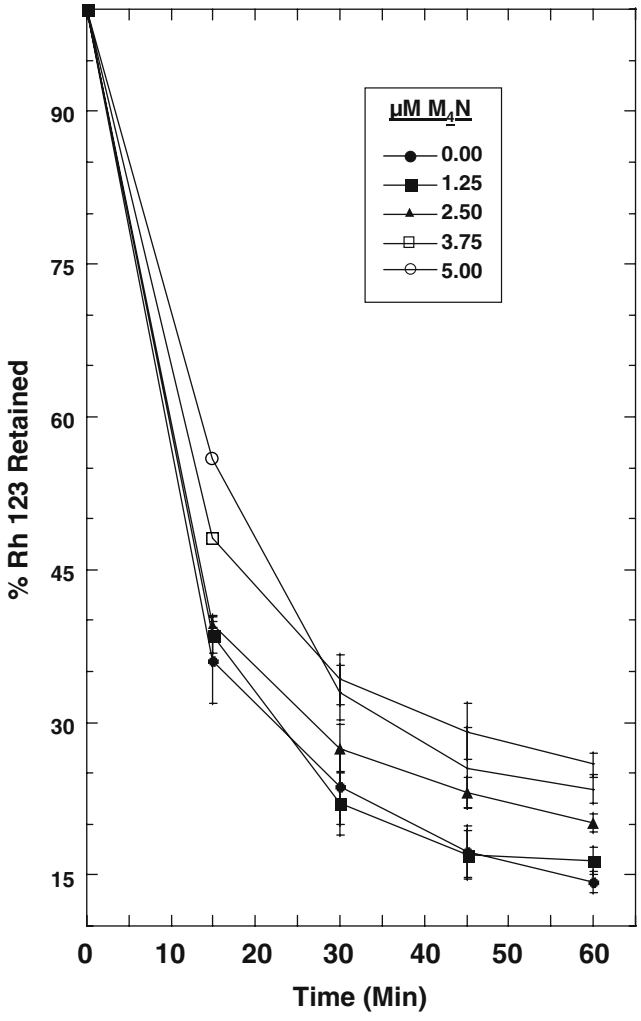

Fig. 7 Inhibition of Pgp-mediated efflux of Rhodamine-123. NCI/ADR-RES cells, incubated for 3 days in the presence of 0, 1.25, 2.5, 3.75, and 5.0 μM M_4N, were tested for their ability to retain Rhodamine-123 as described in Materials and Methods. The percent Rhodamine-123 remaining in the cells was plotted against time

The cytotoxic nature of M_4N also adds complexity to the interpretation of the MDR1 inhibition data. It could be reasoned that the M_4N-induced decreases in MDR1 mRNA and Pgp levels are simply a nonspecific consequence of cellular injury or death. There are several reasons to reject this interpretation. Doxorubicin and paclitaxel act by inhibiting DNA replication and mitosis, respectively. For M_4N to increase their effectiveness, the treated cells must be capable of carrying out these vital processes during the time of MDR reversal and subsequent increased drug retention. In addition, our previous studies have demonstrated that methylated NDGAs are selective for a variety of Sp1-regulated viral and cellular genes [9, 12, 30–33]. The number of genes affected by M_4N has not been determined; however, we have been able to significantly reverse M_4N-induced cell arrest and apoptosis simply by resupplying the cells with CDC2 or survivin [12].

Transcriptional inhibition of MDR1 gene expression is likely not the only component responsible for the MDR reversal effect of M_4N. The effects of M_4N on MDR reversal are clearly multifactorial and other factors such as its inherent toxicity and effect on Pgp stability are probably equally important. The turnover rate of Pgp has important implications for the treatment of multidrug resistant cancers. Pgp appears to be a very stable protein with a half-life of 48–72 h in cultured cells [34]. In our study, 3 days of treatment with 10 μM M_4N reduced the level of Pgp in multidrug resistant cells to approximately 20% of the level in untreated cells. MDR1 mRNA levels were also inhibited, but much less significantly, suggesting M_4N is modulating the stability of Pgp in the treated cells. We have demonstrated previously that M_4N decreases the stability of the IAP survivin by inhibiting its phosphorylation by CDC2 kinase [12]. A recent study of Pgp stability using an MDR-EGFP gene fusion showed that cell surface Pgp is more stable than the newly synthesized cellular form [35]. It could be that M_4N inhibits transport of Pgp to the cell surface, decreasing the stability of the nascent Pgp pool, a possibility that we have yet to investigate, however our results of Pgp antibody staining in M_4N-treated tumors contradict this hypothesis as Pgp levels are decreased even within the interior of the cells.

Other attempts have been made to develop agents that selectively inhibit MDR1 gene expression. Most notable of these are the use of new genetic technologies

Table 2 Effect of M_4N, Maltose-M_3N and paclitaxel, alone and in combination, on the growth of NCI/ADR-RES xenografts

Group	Dosage ($\mu mol/m^2$)	Route	Mean body weight change (g/mouse)	Deaths	Tumors	Relative Mean Tumor Volume	T/C %
Control	0	i.p.	0.0	0/7	14	2.62 ± 0.32	
M_4N	320	i.p.	− 0.2	0/7	14	1.33 ± 0.19	50.8
Px	16	i.p.	− 0.9	0/7	11	1.59 ± 0.25	60.7
M_4N + Px	320 + 16	i.p.	+ 0.3	0/7	8	0.94 ± 0.20	35.9
M4N	160	i.p.	+ 0.2	0/7	13	1.70 ± 0.36	64.9
Px	8	i.p.	+ 0.3	0/7	12	0.90 ± 0.26	34.4
M_4N + Px	160 + 8	i.p.	+ 1.3	0/7	11	0.82 ± 0.11	31.3
Mal-M_3N	320	i.p.	+ 0.6	0/7	13	1.25 ± 0.54	47.7
Mal-M_3N + Px	320 + 16	i.p.	+ 0.2	0/7	14	0.65 ± 0.17	24.8

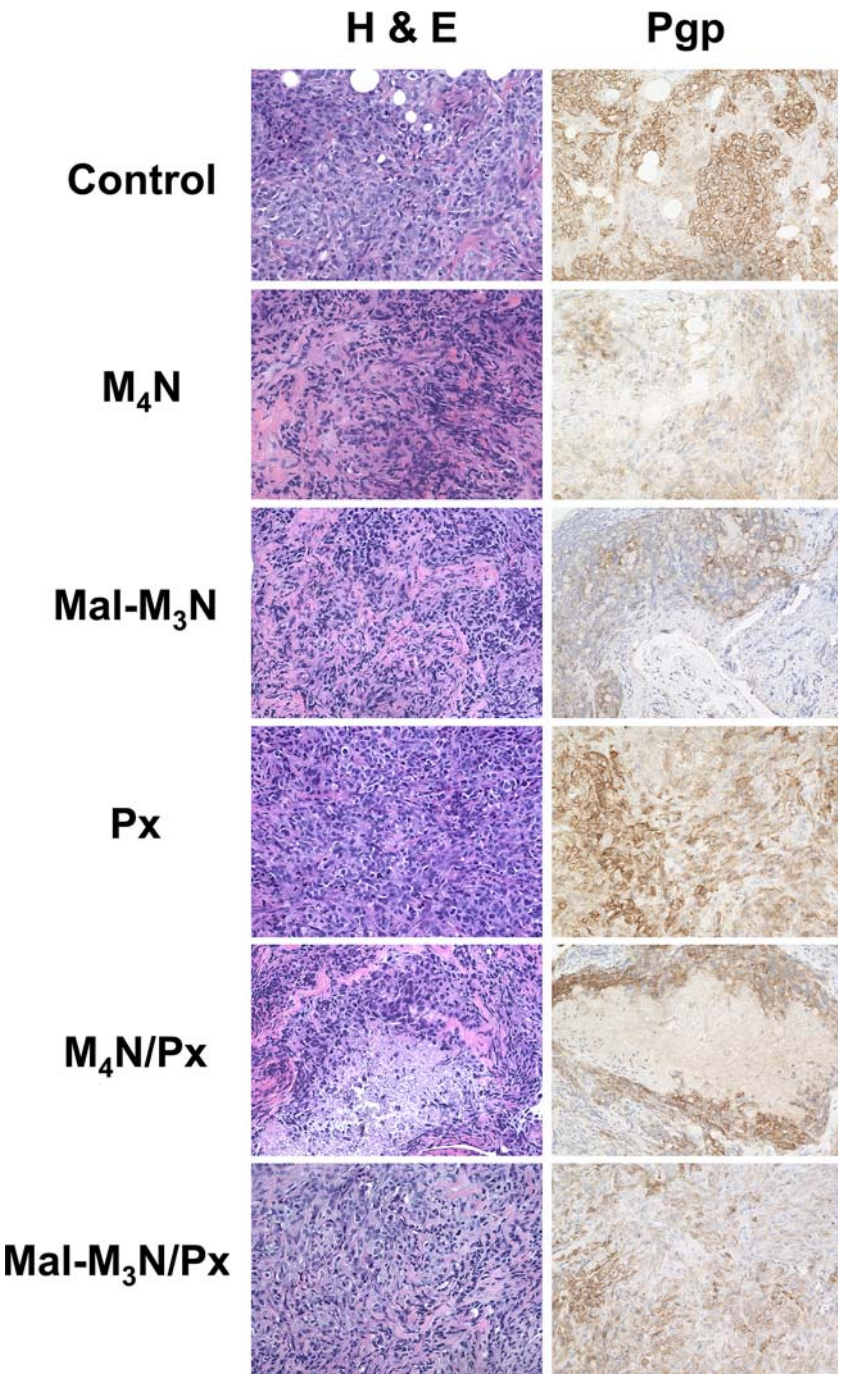

Fig. 8 Effect of M_4N and maltose-M_3N (Mal-M_3N), alone and in combination with paclitaxel (Px), on Pgp protein levels of NCI/ADR-RES breast cancer xenograft tumors in nude mice (online figure in color). Formaldehyde fixed tumors from mice treated daily for 2 weeks with i.p. injections of M_4N (320 μmol/m^2), Mal-M_3N (320 μmol/m^2) or Px (16 μmol/m^2), alone or in combination, were sectioned and analyzed by H&E and immunochemical staining using antibodies specific for human P-glycoprotein (Pgp)

such as antisense oligonucleotides [6], hammerhead ribozymes [7], and small interfering RNAs [8]. While these approaches have had some success in cell culture, the primary challenges for these technologies are achieving delivery to the target tissue and once delivered, fully optimizing expression. We have already demonstrated that, M_4N can be delivered systemically in mice either in a cremophor-based solvent system or orally as part of a corn oil based diet [9], and in this report we have successfully used a newly developed reduced cremophor formulation [24] for i.p. administration. Analogs of M_4N designed to target-specific organ systems are currently being investigated including the water-soluble maltose-M_3N reported here.

Much attention and resources have been directed toward reversing the resistance to multiple anticancer drugs that can develop after courses of adjuvant chemotherapy. With this report, we have demonstrated that M_4N can reverse the MDR phenotype in multidrug resistant human cancer cells. Less attention has been

devoted to preventing the initial development of MDR. We have shown that M_4N also inhibits doxorubicin-mediated induction of MDR1 gene expression raising the possibility that it could be used as a preventative measure. Therefore, we envision several ways M_4N could be utilized as part of an effective strategy for adjuvant chemotherapy in breast and other cancers. Patients whose cancers have become resistant to multiple anticancer agents could be treated with M_4N to reverse the MDR phenotype of the cells, followed by retreatment with agents like doxorubicin or paclitaxel. Another scenario might be the addition of low doses of M_4N to the original adjuvant chemotherapy regimen to prevent the development of MDR. Preclinical studies designed to test these possible treatment regimens with human cancer xenografts are currently in progress.

Acknowledgements This study is supported by grant P690-C25-2407 from Erimos Pharmaceuticals LLC to RCH. The authors would like to thank Theresa Landewe, Mingyu Xi, Chui Cheng and Amy Dinitz for their assistance. YC Liang is a visiting predoctoral fellow from Tunghai University, Taiwan, supported by the National Science Council, Taiwan, R.O.C. CIL and CFL are visiting predoctoral students from National Tsing Hua University, Taiwan.

References

1. Gottesman MM, Fojo T, Bates SE (2002) Multidrug resistance in cancer: role of ATP-dependent transporters. Nat Rev Cancer 2:48–58
2. Minotti G, Menna P, Salvatorelli E, Cairo G, Gianni L (2004) Anthracyclines: molecular advances and pharmacologic developments in antitumor activity and cardiotoxicity. Pharmacol Rev 56:185–229
3. Abal M, Andreu JM, Barasoain I (2003) Taxanes: microtubule and centrosome targets, and cell cycle dependent mechanisms of action. Curr Cancer Drug Targets 3:193–203
4. Thomas H, Coley HM (2003) Overcoming multidrug resistance in cancer: an update on the clinical strategy of inhibiting p-glycoprotein. Cancer Control 10:159–165
5. Haus-Cohen M, Assaraf YG, Binyamin L, Benhar I, Reiter Y (2004) Disruption of P-glycoprotein anticancer drug efflux activity by a small recombinant single-chain Fv antibody fragment targeted to an extracellular epitope. Int J Cancer 109:750–758
6. Kang H, Fisher MH, Xu D, Miyamoto YJ, Marchand A, Van Aerschot A, Herdewijn P, Juliano RL (2004) Inhibition of MDR1 gene expression by chimeric HNA antisense oligonucleotides. Nucleic Acids Res 32:4411–4419
7. Nagata J, Kijima H, Hatanaka H, Asai S, Miyachi H, Abe Y, Yamazaki H, Nakamura M, Watanabe N, Mine T, Kondo T, Scanlon KJ, Ueyama Y (2002) Reversal of drug resistance using hammerhead ribozymes against multidrug resistance-associated protein and multidrug resistance 1 gene. Int J Oncol 21:1021–1026
8. Xu D, Kang H, Fisher M, Juliano RL (2004) Strategies for inhibition of MDR1 gene expression. Mol Pharmacol 66:268–275
9. Park R, Chang C-C, Liang Y-C, Chung Y, henry RA, Lin E, Mold De, Huang RCC (2005) Systemic treatment with tetra-O-methyl nordihydroguaiaretic acid suppresses the growth of human xenograft tumors. Clin Cancer Res 11:4601–4609
10. Lin E (2003) The prospect of tetra-*O*-methyl nordihydroguaiaretic acid (M_4N) as a systemically delivered chemotherapeutic agent. M.Sc. thesis, Johns Hopkins University
11. Data on file, Erimos Pharmaceutical, LLC, Raleigh, North Carolina
12. Chang CC, Heller JD, Kuo J, Huang RC (2004) Tetra-O-methyl nordihydroguaiaretic acid induces growth arrest and cellular apoptosis by inhibiting Cdc2 and survivin expression. Proc Natl Acad Sci USA 101:13239–13244
13. Heller JD, Kuo J, Wu TC, Kast WM, Huang RC (2001) Tetra-*O*-methyl nordihydroguaiaretic acid induces G2 arrest in mammalian cells and exhibits tumoricidal activity in vivo. Cancer Res 61:5499–5504
14. Greijer AE, van der Groep P, Kemming D, Shvarts A, Semenza GL, Meijer GA, van de Weil MA, Belien JA, van Diest PJ, van der Wall E (2005) Up-regulation of gene expression by hypoxia is mediated predominantly by hypoxia-inducible factor 1 (HIF-1). J Pathol 206:291–304
15. Scotto KW (2003) Transcriptional regulation of ABC drug transporters. Oncogene 22:7496–7511
16. Adams S, Robbins F-M, Chen D, Wagage D, Holbeck SL, Morse III HC, Stroncek D, Marincola FM (2005) HLA class I and II genotype of the NCI-60 cell lines. J Transl Med 3:11–18
17. >Hwu JR, Tseng WN, Gnabre J, Giza P, Huang RC (1998) Antiviral activities of methylated nordihydroguaiaretic acids. 1. Synthesis, structure identification, and inhibition of tat-regulated HIV transactivation. J Med Chem 41:2994–3000
18. Skehan P, Storeng R, Scudiero D, Monks A, McMahon J, Vistica D, Warren JT, Bokesch H, Kenney S, Boyd MR (1990) New colorimetric cytotoxicity assay for anticancer-drug screening. J Natl Cancer Inst 82:1107–1112
19. Chou TC, Talalay P (1984) Quantitative analysis of dose–effect relationships: the combined effects of multiple drugs or enzyme inhibitors. Adv Enzyme Regul 22:27–55
20. Chang TT, Chou TC (2000) Rational approach to the clinical protocol design for drug combinations: a review. Acta Paediatr Taiwan 41:294–302
21. Chou TC (1991) The median effect principle and the combination index for quantitation of synergism and antagonism. In: Chou TC, Rideout DC (eds) Synergism and antagonism in chemotherapy. Academic Press, San Diego, pp 61–102
22. Chou TC, Motzer RJ, Tong Y, Bosl GJ (1994) Computerized quantitation of synergism and antagonism of taxol, topotecan, and cisplatin against human teratocarcinoma cell growth: a rational approach to clinical protocol design. J Natl Cancer Inst 86:1517–1524
23. Chou TC, Martin N (2005) CompuSyn for Drug Combinations. ComboSyn, Inc. P.O. Box 1277, Paramus, NJ
24. Chao TC, Chu Z, Tseng LM, Chiou TJ, Hsieh RK, Wang WS, Yen CC, Yang MH, Hsiao LT, Liu JH, Chen PM (2005) Paclitaxel in a novel formulation containing less Cremophor EL as first-line therapy for advanced breast cancer: a phase II trial. Invest New Drugs 23:171–177
25. Bissery MC, Guenard D, Gueritte-Voegelein F, Lavelle F (1991) Experimental antitumor activity of taxotere (RP 56976, NSC 628503), a taxol analogue. Cancer Res 51:4845–4852
26. McDaid HM, Lopez-Barcons L, Grossman A, Lia M, Keller S, Perez-Soler R, Horwitz SB (2005) Enhancement of the therapeutic efficacy of taxol by the mitogen-activated protein kinase kinase inhibitor CI-1040 in nude mice bearing human heterotransplants. Cancer Res 65:2854–2860
27. Takahashi N, Li W, Banerjee D, Guan Y, Wada-Takahashi Y, Brennan MF, Chou TC, Scotto KW, Bertino JR (2002) Sequence-dependent synergistic cytotoxicity of ecteinascidin-743 and paclitaxel in human breast cancer cell lines in vitro and in vivo. Cancer Res 62:6909–6915
28. Liao CH, Pan SL, Guh JH, Chang YL, Pai HC, Lin CH, Teng CM (2005) Antitumor mechanism of evodiamine, a constituent from Chinese herb Evodiae fructus, in human multiple-drug resistant breast cancer NCI/ADR-RES cells in vitro and in vivo. Carcinogenesis 26:968–975
29. Chang C-C (2005) Ph.D Thesis, Johns Hopkins University

30. Gnabre JN, Brady JN, Clanton DJ, Ito Y, Dittmer J, Bates RB, Huang RC (1995) Inhibition of human immunodeficiency virus type 1 transcription and replication by DNA sequence-selective plant lignans. Proc Natl Acad Sci USA 92:11239–11243
31. Hwu JR, Tseng WN, Gnabre J, Giza P, Huang RC (1998) Antiviral activities of methylated nordihydroguaiaretic acids. 1. Synthesis, structure identification, and inhibition of tat-regulated HIV transactivation. J Med Chem 41:2994–3000
32. Craigo J, Callahan M, Huang RC, DeLucia AL (2000) Inhibition of human papillomavirus type 16 gene expression by nordihydroguaiaretic acid plant lignan derivatives. Antiviral Res 47:19–28
33. Chen H, Teng L, Li JN, Park R, Mold DE, Gnabre J, Hwu JR, Tseng WN, Huang RC (1998) Antiviral activities of methylated nordihydroguaiaretic acids. 2. Targeting herpes simplex virus replication by the mutation insensitive transcription inhibitor tetra-O-methyl-NDGA. J Med Chem 41:3001–3007
34. Richert ND, Aldwin L, Nitecki D, Gottesman MM, Pastan I (1988) Stability and covalent modification of P-glycoprotein in multidrug-resistant KB cells. Biochemistry 27:7607–7613
35. Petriz J, Gottesman MM, Aran JM (2004) An MDR-EGFP gene fusion allows for direct localization, function and stability assessment of p-glycoprotein. Curr Drug Deliv 1:43–56